

Functionalised Poly(Vinyl Alcohol)/Graphene Oxide as Polymer Composite Electrolyte Membranes

O. Gil-Castell^{1,2}, R. Cerveró¹, R. Teruel-Juanes¹, J. D. Badia^{1,2} and A. Ribes-Greus^{1,*}

¹Instituto de Tecnología de Materiales (ITM), Universitat Politècnica de València (UPV), Camino de Vera s/n, Valencia, Spain.

²Departament d'Enginyeria Química, Escola Tècnica Superior d'Enginyeria, Universitat de València (UV), Av. de la Universitat s/n, Burjassot, Spain.

*Corresponding Author: A. Ribes-Greus. Email: aribes@ter.upv.es.

Abstract: Crosslinked poly(vinyl alcohol) (PVA) based composite films were prepared as polyelectrolyte membranes for low temperature direct ethanol fuel cells (DEFC). The membranes were functionalised by means of the addition of graphene oxide (GO) and sulfonated graphene oxide (SGO) and crosslinked with sulfosuccinic acid (SSA). The chemical structure was corroborated and suitable thermal properties were found. Although the addition of GO and SGO slightly decreased the proton conductivity of the membranes, a significant reduction of the ethanol solution swelling and crossover was encountered, more relevant for those functionalised with SGO. In general, the composite membranes were stable under simulated service conditions. The addition of GO and SGO particles permitted to buffer the loss and almost retain similar proton conductivity than prior to immersion. These membranes are alternative polyelectrolytes, which overcome current concerns of actual commercial membranes such as the high cost or the crossover phenomenon.

Keywords: Direct ethanol fuel cell; graphene oxide; poly(vinyl alcohol); proton exchange membranes; proton conductivity

1 Introduction

Composite materials have received great attention as a feasible alternative with great potential for application as polymer electrolyte membranes (PEMs) in direct ethanol fuel cells (DEFCs) [1]. The PEM must possess high proton conductivity and fuel selectivity to prevent the crossover phenomenon. As polymer matrix, poly(vinyl alcohol) (PVA) is a synthetic water soluble non-toxic polymer, which has been extensively used as alcohol dehydrating agent due to its high water/alcohol selectivity. Taking advantage of this performance, PVA is an attractive material for PEM preparation [2,3]. However, due to the absence of negatively charged ions, it is a poor proton conductor, which requires functionalisation in order to promote the required features for being used as PEM [4].

The combination of poly(vinyl alcohol) (PVA) with sulfosuccinic acid (SSA) is one of the best alternatives for providing high stability due to the cross-linked structure and favouring the proton conductivity. The presence of SSA in the PEM structure introduces a negative charged ion group (sulfonic), which will play a key role in the proton transport [5]. As well, with the aim to improve the crossover resistance, reduce the fuel permeability, and enhance the proton conductivity, the PVA is frequently filled with organic or inorganic particles [6].

The combination of PVA and SSA with nano-scaled particles such as graphene oxide (GO) can be considered as a feasible pathway for the preparation of polymer electrolyte membranes [7,8]. The incorporation of functionalised nanoparticles aims to combine the advantages of inorganic materials, such as the thermal and dimensional stability, and those of polymers, such as conductivity and flexibility, that

overcome the existing limitations with lower cost and high functional performance [9]. On the one hand, at high temperatures, the inorganic particles that are proton conductors embedded into the polymer matrix increase their conductivity and, when the matrix is properly hydrated, they act as a bridge to connect adjacent ionic groups [10,11]. That is the reason why the inorganic particles must not agglomerate forming blockages in the hydrophilic channels. On the other hand, the incorporation of nanoparticles to the membrane may reduce the fuel crossover. The fuel permeation is produced by diffusion through pores or holes as well as through hydrophilic channels. The addition of inorganic particles that block the holes or transport routes intends to reduce the fuel permeability and subsequent crossover. In this way, a suitable balance between good proton conductivity and low fuel permeability can be achieved [9].

Graphene oxide (GO) has a unique two-dimensional structure with excellent dimensional, chemical and thermal stability, low permeability, low cost, surface functionality and minimum thickness [7]. One of the keys of the GO is that it can be produced from graphite using several oxidation routes in a relatively easy way [12]. The GO structure consists of carbons connected to each other by covalent bonds and interconnected to hydrogen and oxygen, to form a structure stratified with epoxy, hydroxyl and carboxyl groups in the basal plane and at the edge for providing a high specific surface area. The presence of such groups provides the structure with high functionality and excellent capacity to interact with various materials, such as the PVA matrix and the SSA crosslinking agent.

In this line, the addition of graphene oxide (GO) and sulfonated graphene oxide (SGO) to the membranes must be assessed in terms of the physico-chemical characterisation along with the evaluation of the proton conductivity, essential for DEFC applications. In parallel, the assessment of the fuel uptake ability and the ethanol crossover will bring valuable information for its application as PEMs. Finally, the study of the hydrolytic stability under simulated service conditions in terms of macroscopic appearance, thermo-oxidative stability, thermal properties and proton conductivity as a function of the immersion time in simulated working conditions was considered necessary for an appropriate application.

2 Materials and Methods

2.1 Materials

Poly(vinyl alcohol) (PVA) (99% hydrolysed, $M_w = 130000 \text{ g}\cdot\text{mol}^{-1}$) and 70% sulfosuccinic acid (SSA), were purchased from Sigma Aldrich; absolute ethanol ($\text{C}_2\text{H}_5\text{OH}$) from Scharlau. Ultra-pure water was obtained from an ultra-filtration/ion-exchange procedure. Graphene oxide (GO) and sulfonated GO (SGO) were obtained by the modified Hummers method [12], and functionalised [13,14].

2.2 Membrane Preparation

The membranes were obtained by means of a solvent-casting procedure and further crosslinked by compression moulding at 120°C to achieve dimensional control. For this purpose, a PVA solution was prepared in water (15 %wt) at 90°C for 6 h. Then, a 30 %wt_{PVA} of SSA was added and, afterwards, sonicated GO and SGO solutions were incorporated to the membranes to achieve concentrations, ranging from 0.25 to 1.00 %wt_{PVA}.

2.3 Membrane Characterisation and Validation

2.3.1 Fourier Transformed Infrared Spectroscopy (FTIR)

The chemical structure of membranes was evaluated by means of a Thermo Nicolet 5700 in a attenuated total reflectance (ATR) setup. The IR spectra was assessed between 4000 and 400 cm^{-1} with a resolution of 4 cm^{-1} along 64 accumulations.

2.3.2 Differential Scanning Calorimetry (DSC)

DSC was performed into a Mettler Toledo DSC 822° equipped with a cooling system. Samples between 3 and 5 mg were placed into 40 μL Al crucibles. Three consecutive heating-cooling-heating segments from 50°C to 250°C with a heating/cooling rate of 10 $^{\circ}\text{C}\cdot\text{min}^{-1}$ were performed under inert N_2 atmosphere at a flow rate of 50 $\text{mL}\cdot\text{min}^{-1}$.

2.3.3 Thermogravimetry (TGA)

The samples, with a mass between 3 and 5 mg, were introduced into 70 μL alumina capsules. The samples were then placed in the Mettler Toledo TGA 851 analyser and subjected to a dynamic test, from 25°C to 800°C with a heating rate of 10 $^{\circ}\text{C}\cdot\text{min}^{-1}$. The tests were carried out under an O_2 atmosphere with at a flow rate of 50 $\text{mL}\cdot\text{min}^{-1}$.

2.3.4 Ethanol Solution Uptake

Membrane samples of about $1 \times 1 \text{ cm}^2$ were immersed into 20 mL of 2 M ethanol solution and placed in test tubes into a Selecta Unitronic Bath at 40°C. The solution absorption was monitored gravimetrically up to 65 days of immersion according to the Eq. (1), where m_t was the mass measured after each stage of immersion and m_0 the initial mass of the membranes.

$$M_t(\%) = \frac{m_t - m_0}{m_0} \times 100 \quad (1)$$

2.3.5 Ethanol Permeability

The ethanol permeability of the membranes was evaluated by means of a glass diffusion cell with two reservoirs, each of 1 L of capacity. Pre-hydrated membranes immersed in water for 24 h were sandwiched between the two modules that contained deionised water and 2 M ethanol solution, respectively. The solutions were magnetically stirred and thermostatically controlled at 40°C. The permeability was indirectly measured from the electric conductivity variation of the water reservoir, which signals were processed with the LabView software as a function of time. For this purpose, the relative conductivity ($cond_{rel}$) was defined according to the Eq. (2), where $cond_t$ is the conductivity as a function of time and $cond_0$ is the initial conductivity.

$$cond_{rel}(\%) = \frac{cond_t}{cond_0} \times 100 \quad (2)$$

2.3.6 Proton Conductivity

The proton conductivity (σ_{prot}) was measured in an alpha mainframe frequency analyser in conjunction with an active cell (Concept 40, Novocontrol Technologies BmgH & Co.). The response was measured from 10^{-2} to 10^7 Hz, at room temperature (25°C). The sample electrode assembly (SEA) consisted in two stainless steel electrodes filled with the polymer. The diameters of the electrodes were 20 mm and the thickness was kept around 30 μm . The membranes were fully hydrated with ultra-pure water for 24 h. The σ_{prot} ($\text{S}\cdot\text{cm}^{-1}$) of the membranes was calculated according to the Eq. (3).

$$\sigma_{prot} = \frac{l}{A \cdot R_0} \quad (3)$$

where l is the thickness of the conducting membranes in cm, A the area of the electrode in contact with the membrane in cm^2 , and R_0 the protonic resistance taken from the Bode plot at high frequencies in ohms (Ω) [15].

2.3.7 Hydrolytic Stability

The hydrolytic stability of the membranes was studied during immersion for several long-term stages. Accordingly, samples were removed after 7, 14, 28, 56 and 100 days, and dried under vacuum at 30°C for

48 h. The ethanol solution was replaced once a week in order to preserve it fresh. The changes after immersion were characterised in terms of the variation of the macro and microscopic appearance, the thermal properties and the thermo-oxidative stability. As well, the proton conductivity was measured after 100 days of immersion.

3 Results and Discussion

3.1 Physico-Chemical Characterisation

The proposed membranes were physico-chemically characterised in terms of chemical structure, thermo-oxidative stability, thermal properties and proton conductivity for assuring their suitability for polyelectrolyte applications in DEFCs. Macroscopically, the membranes revealed an intense brownish and rigid appearance after crosslinking, regardless the composition. The generation of sulphuric acid cues from the sulfosuccinic acid (SSA) during the crosslinking reaction may have been the cause of this change [16].

The chemical composition of the PVA, PVA/SSA and GO components and PVA/SSA/GO and PVA/SSA/SGO membranes was assessed, which FTIR spectra are plotted in Fig. 1. The PVA membranes showed a broad band between 3400 and 3000 cm^{-1} , associated to the hydroxyl group stretching (-OH) of intra and intermolecular interactions and retained water molecules. Moreover, the peaks between 3000-2800 cm^{-1} and 1500-1300 cm^{-1} corresponded to the stretching and bending of the $-\text{CH}_2-$ of the PVA backbone [17]. The addition of SSA was perceived in the 1780 and 1710 cm^{-1} bands associated to the carboxyl (-COOH) and acetate (-COO-) groups and corroborated in the peak at 1040 cm^{-1} , correlated with sulfonic groups (-SO₃H) [18]. The GO showed the characteristic peaks at 3450, 1720, 1600, 1400 and 1100 cm^{-1} , which can be correlated to hydroxyl stretching (-OH), carboxyl stretching (C=O), backbone of non-oxidised graphite and C=C bond, and bending of (O-H) and (C-O) of hydroxyl groups, respectively [19]. However, due to the low concentration of the GO in the composites, the bands of these particles were overlapped in the spectra of the membranes. As well, the absence of the GO peaks can be associated to a satisfactory particle dispersion. On the other hand, the incorporation of SGO to the membranes resulted in higher intensity of the signals associated to the sulfonic group and, thus, corroborating the higher sulfonation degree of these membranes, higher as SGO content increased.

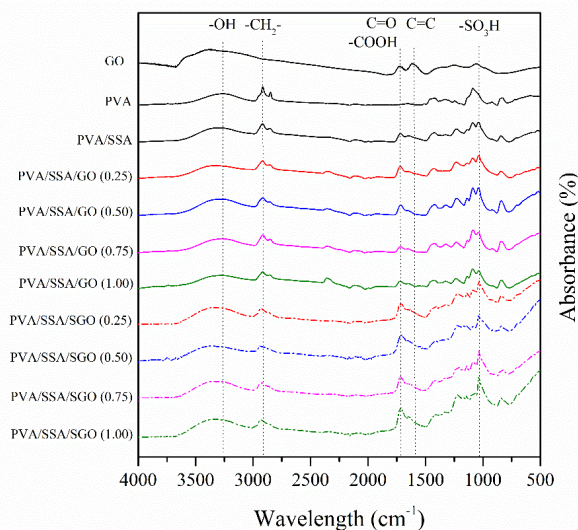


Figure 1: FTIR spectra of the PVA/SSA/GO and PVA/SSA/SGO membranes

The study of the thermo-oxidative stability of the pure PVA membrane revealed the typical two-step mass loss behaviour, as shown in Fig. 2. The first step, until 200°C, involved the free water evaporation (~5%), which has no strong interaction within the polymer molecules. Then, the degradation of side groups from the main chain and the loss of bound water was observed between 230 and 400°C. This stage involved the elimination of chemically bounded water, mainly by means of hydrogen bonding, and hydroxyl groups (-OH) that promoted a polyene structure, chain scission and cyclization reactions. Finally, above 400°C, the degradation of the polymer backbone took place [18]. In the PVA/SSA-based crosslinked membranes, a multi-stage decomposition behaviour was perceived. Free water was released between 50 and 100°C, followed by the release of bound water in the region from 100 to 230°C, and also water generated as a product of further esterification reactions between the remnant hydroxyl groups from PVA and carboxyl groups from SSA molecules. Then, the sulfonic group (-SO₃H) decomposition and the ester bond scission were found between 230 and 350°C. Finally, above 400°C, the decomposition of the PVA backbone was observed [20]. If compared to pure PVA, this stage was more pronounced for the PVA/SSA-based membranes and moved towards higher temperatures. Moreover, residual mass values increased from ~2 to ~15%. These changes can be explained by the highly crosslinked structure of these materials [18]. For the PVA/SSA/GO and PVA/SSA/SGO composites, similar thermogravimetric curves were perceived. The thermo-oxidative stability of the composite membranes remained basically constant, regardless the presence of the GO or SGO particles (< 1%).

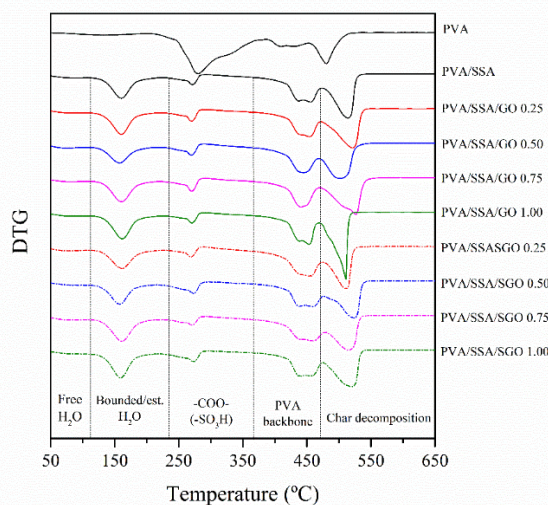


Figure 2: Derivative thermo-gravimetric (DTG) curves of the PVA, PVA/SSA, PVA/SSA/GO and PVA/SSA/SGO membranes

The thermal properties were furtherly evaluated by means of differential scanning calorimetry. The obtained calorimetric traces of the first heating scan are plotted in Fig. 3. The pure PVA showed a wide endotherm from 40 to 80°C that involved the release of free water. Then, a melting peak was found around 210°C. However, for the crosslinked PVA/SSA-based membranes, a wide bimodal endotherm from 40 to 180°C was observed. These peaks can be correlated to those observed in the TGA analysis. The first peak, around 90°C, is ascribed to the free water release. Accordingly, the peak around 160°C involved the release of bound water and water produced by further esterification reactions. The addition of GO and SGO particles, slightly moved these events towards higher temperatures (1-2°C). Given this behaviour, it seems that the thermal properties were unaltered by the addition of GO and SGO particles. From the second heating scan, the pure PVA revealed a glass transition around 123°C. However, a flat thermogram was obtained for the composite membranes, in which the step change associated with the T_g could not be

perceived. This phenomenon may suggest a compact and crosslinked structure of the composite membranes that prevented the observation of the PVA glass transition [21].

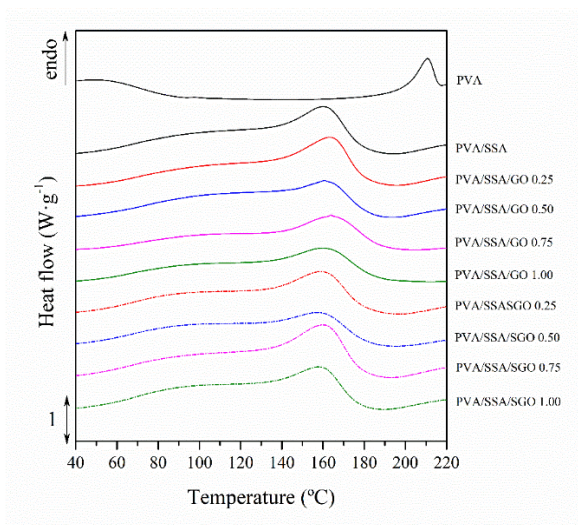


Figure 3: Calorimetric thermograms of the first heating scan of the PVA, PVA/SSA, PVA/SSA/GO and PVA/SSA/SGO membranes

3.2 Ethanol Solution Absorption

The membranes were immersed into 2 M ethanol solutions at 40°C and gravimetrically monitored as a function of the immersion time. The mass variation until saturation is plotted in Fig. 4. The ethanol solution penetrated into the membranes and the overall mass increased. The PVA/SSA membrane swelled up to 40% of ethanol solution. As the GO content increased, the solution uptake decreased. The GO may have hindered the advance of penetrant along the membrane, which will contribute to reduce the ethanol crossover. Moreover, the functional groups of the GO may have interacted with the PVA and SSA molecules, giving rise to a more compact structure with less free volume available for the penetrant. When SGO was incorporated, this behaviour was emphasised, and the global solution uptake was lower than that of the GO-based membranes.

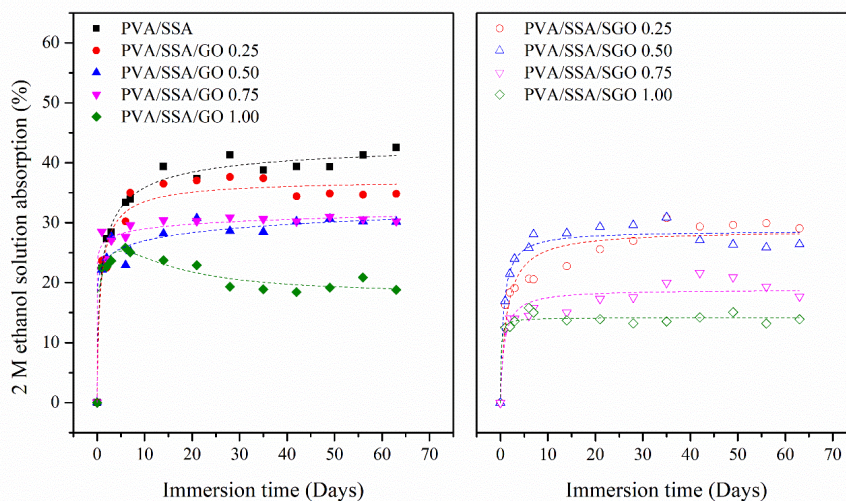


Figure 4: Ethanol solution absorption profiles of the PVA/SSA, PVA/SSA/GO (left) and PVA/SSA/SGO (right) membranes. Error bars were omitted for the sake of clarity

3.3 Ethanol Permeability

The ethanol permeability was evaluated from the relative electric conductivity ($cond_{rel}$) variation between two reservoirs of water and 2 M ethanol solution as a function of time. The obtained permeation curves for the PVA/SSA/GO based hydrated membranes are plotted in Fig. 5. The relative conductivity remained almost constant for the PVA-based membranes. Indeed, it slightly increased due to the ambient CO₂ diluted in the reservoir along the experiment. The addition of GO and SGO nanoparticles in the composite membranes seemed to have prevented them from ethanol permeation. Given these results, membranes can be considered as impermeable to ethanol under the usual service conditions, in comparison to Nafion® 117 membrane, which is one of the main drawbacks of this extended commercial membrane [22].

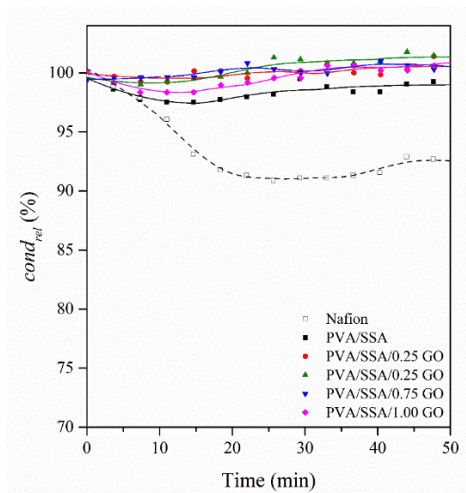


Figure 5: Relative variation of the conductivity for the PVA/SSA/GO and the Nafion® 117 membranes. Error bars were omitted for the sake of clarity

3.4 Proton Conductivity

The proton conductivity (σ_{prot}) of the membranes was assessed at 25°C, which results are gathered in Tab. 1. The addition of GO to the membranes reduced the σ_{prot} . Although the analyses were carried out after 24 h of immersion in water to guarantee proper hydration, the low thickness of the membranes (30 μm) may have resulted in lower hydration degree and high desorption rate of swelled humidity, which is crucial for proton transport through the membrane [23,24]. As well, the addition of GO nanoparticles seemed to have promoted a highly compact structure that reduced the hydration ability and hindered the proton transport pathways. However, when SGO was added, the proton conductivity moderately decreased. The contribution of the sulfonic groups grafted to the SGO particles may have enhanced the proton transport by means of the generation of more proton transport pathways and buffered the decrease of the proton conductivity.

Table 1: Proton conductivity of the PVA/SSA, PVA/SSA/GO and PVA/SSA/SGO membranes






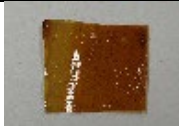












σ_{prot} ($\text{mS}\cdot\text{cm}^{-1}$)	PVA/SSA	
	0.5861 ± 0.0297	
	PVA/SSA/GO	PVA/SSA/SGO
0.25	0.4691 ± 0.0442	0.3715 ± 0.0212
0.50	0.1459 ± 0.0502	0.4406 ± 0.0538
0.75	0.0520 ± 0.0288	0.1146 ± 0.0113
1.00	0.0915 ± 0.0102	0.1347 ± 0.0225

3.5 Hydrolytic Stability Under Simulated Service Conditions

The evaluation of the hydrolytic stability of the membranes under simulated service conditions was performed, which can be closely related to their performance for being applied as electrolytes in fuel cell applications. For this purpose, membranes were characterised during several immersion stages into 2 M ethanol solution and evaluated in terms of appearance, thermo-oxidative stability, thermal properties and proton conductivity.

The blackish original membranes turned clearer after 100 days of immersion. This change was more perceivable for the PVA/SSA membrane and those membranes that contained SGO, as shown in Tab. 2.

Table 2: Macroscopic appearance after 100 days of immersion

		PVA/SSA			
		Day 0		Day 100	
-					
GO (%wt)	PVA/SSA/SGO				
	Day 0	Day 100	Day 0	Day 100	
0.25					
0.50					
0.75					
1.00					

The thermo-oxidative stability analyses revealed that the peak associated to the release of bound water and water molecules generated by remnant crosslinking reactions lost importance and moved towards higher temperatures along immersion in all cases. On the one hand, residual esterification reactions may have been completed during immersion, which contribution during the TGA analysis disappeared. On the other hand, higher immersion time may have promoted better water-polymer interaction that needed more temperature to be released. This observation was also visible in the calorimetric results. Moreover, the thermo-oxidative stability evaluation showed a considerable reduction of the desulfonation peak in the DTG curve. Unreacted SSA molecules may have leached from the membrane to the surrounding media. This observation was perceivable from the first stage of immersion. Finally, the peak that involved the backbone decomposition of the PVA moved to lower temperatures as the immersion time increased. Highly swelled membranes after 100 days of immersion may have left more free volume through which oxygen molecules diffused and promoted lower thermo-oxidative stability. As an example of these observations, the thermogravimetric and its derivative curves, along with calorimetric thermograms are shown in Fig. 6 as a function

of the immersion time for the PVA/SSA/GO 0.75 membrane. The behaviour perceived for the other membranes was similar, regardless the presence of GO or SGO.

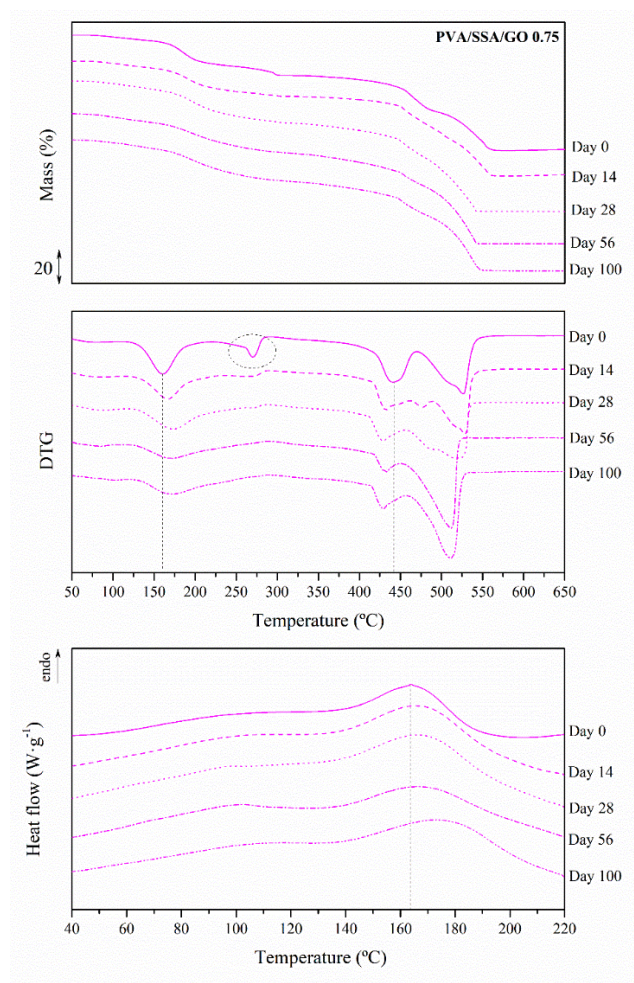


Figure 6: TGA, DTG and calorimetric traces for the PVA/SSA/GO 0.75 membrane as a function of the immersion time

The proton conductivity (σ_{prot}) was also assessed in the membranes after immersion in 2 M ethanol solution and results are gathered in Tab. 3. The σ_{prot} considerably decreased after immersion in all cases. While this decrease was dramatic for the PVA/SSA membranes, the reduction in those containing a 0.50% of GO/SGO was buffered to some extent and the conductivity results for those with 0.75% of GO/SGO were comparable to that before immersion. The suitability of these amounts of GO-based fillers for fuel cell applications has been suggested before [14]. In general, the membranes containing SGO revealed a slightly higher conductivity after immersion than those including GO. The crosslinking between the PVA, the SSA and the GO and especially SGO particles may have contributed to preserve the proton conductivity after immersion by means of the creation of stable and permanent proton transport pathways in these composite structures.

Table 3: Proton conductivity after 100 days of immersion

σ_{prot} (mS·cm ⁻¹)	PVA/SSA	
	0.0041 ± 0.0007	
	PVA/SSA/GO	PVA/SSA/SGO
0.25	0.0032 ± 0.0009	0.0044 ± 0.0010
0.50	0.0410 ± 0.0045	0.0684 ± 0.0098
0.75	0.0388 ± 0.0087	0.0741 ± 0.0102
1.00	0.0131 ± 0.0021	0.0193 ± 0.0055

4 Conclusions

The combination of a solvent-casting and thermal crosslinking procedure resulted in an effective mode to produce functionalised PVA/SSA/GO and PVA/SSA/SGO composite polyelectrolyte membranes. Although the addition of GO and SGO slightly reduced the proton conductivity, a reduction of the ethanol solution swelling and crossover was found. This behaviour was more significant for the SGO functionalized membranes, which showed high barrier effect against the ethanol crossover.

The membranes subjected to simulated service conditions were stable after long-term evaluation. Although the proton conductivity decreased due to the probable deprotonation during immersion, the addition of GO/SGO (0.50% and especially 0.75 %wt.) permitted to buffer the reduction and revealed comparable values to that found prior to immersion. In this sense, the addition of SGO was more effective and makes these membranes a promising alternative in the DEFC field.

Acknowledgments: The authors would like to thank the support of the European Union through the European Regional Development Funds (ERDF). The Spanish Ministry of Economy, Industry and Competitiveness, is thanked for the research project POLYDECARBOCELL (ENE2017-86711-C3-1-R). The Spanish Ministry of Education, Culture and Sports is thanked for the FPU grant for O. Gil-Castell (FPU13/01916).

References

1. Vaghari, H., Jafarizadeh-Malmiri, H., Berenjian, A., Anarjan, N. (2013). Recent advances in application of chitosan in fuel cells. *Sustainable Chemical Processes*, 1, 16.
2. Chiang, W. Y. (1998). *Separation of water-alcohol mixture by using polymer membranes*. Taiwan, R.O.C.: Elsevier Science Pub. Co.
3. Pivovar, B. S., Wang, Y. X., Cussler, E. L. (1999). Pervaporation membranes in direct methanol fuel cells. *Journal of Membrane Science*, 154, 155-162.
4. Ye, Y. S., Rick, J., Hwang, B. J. (2012). Water soluble polymers as proton exchange membranes for fuel cells. *Polymers (Basel)*, 4, 913-963.
5. Meenakshi, S. Bhat, S. D., Sahu, A. K., Sridhar, P., Pitchumani, S. et al. (2012). Chitosan-polyvinyl alcohol-sulfonated polyethersulfone mixed-matrix membranes as methanol-barrier electrolytes for DMFCs. *Journal of Applied Polymer Science*, 124, 73-82.
6. Moore, T. T., Mahajan, R., Vu, D. Q., Koros, W. J. (2004). Hybrid membrane materials comprising organic polymers with rigid dispersed phases. *AIChE Journal*, 50, 311-21.
7. Farooqui, U. R., Ahmad, A. L., Hamid, N. A. (2018). Graphene oxide: a promising membrane material for fuel cells. *Renewable and Sustainable Energy Reviews*, 82(1), 714-733.
8. Pandey, R. P., Shukla, G., Manohar, M., Shahi, V. K. (2016). Graphene oxide based nanohybrid proton exchange membranes for fuel cell applications: an overview. *Advances in Colloid and Interface Science*, 240, 15-30.
9. Nunes, S., Ruffmann, B., Rikowski, E., Vetter, S., Richau, K. (2002). Inorganic modification of proton

- conductive polymer membranes for direct methanol fuel cells. *Journal of Membrane Science*, 203, 215-25.
10. Chung, T. S., Jiang, L. Y., Li, Y., Kulprathipanja, S. (2007). Mixed matrix membranes (MMMs) comprising organic polymers with dispersed inorganic fillers for gas separation. *Progress in Polymer Science*, 32, 483-507.
 11. Miyake, N., Wainright, J. S., Savinell, R. F. (2001). Evaluation of a sol-gel derived nafion/silica hybrid membrane for proton electrolyte membrane fuel cell applications: I. Proton conductivity and water content. *Journal of the Electrochemical Society*, 148, 898-904.
 12. Hummers, W. S., Offeman, R. E. (1958). Preparation of graphitic oxide. *Journal of the American Chemical Society*, 80, 1339-1339.
 13. Sánchez Ballester, S. C. (2017). *Synthesis and characterization of new polymer electrolytes to use in fuel cells fed with bio-alcohols*. Universitat Politècnica de València.
 14. González-Guisasola, C., Ribes-Greus, A. (2018). Dielectric relaxations and conductivity of cross-linked PVA/SSA/GO composite membranes for fuel cells. *Polymer Testing*, 67, 55-67.
 15. Qian, X., Gu, N. Y., Cheng, Z. L., Yang, X. R., Wang, E. K. et al. (2001). Methods to study the ionic conductivity of polymeric electrolytes using a.c. impedance spectroscopy. *Journal of Solid State Electrochemistry*, 6, 8-15.
 16. Xie, B., Hong, L., Chen, P., Zhu, B. (2016). Effect of sulfonation with concentrated sulfuric acid on the composition and carbonizability of LLDPE fibers. *Polymer Bulletin*, 73, 891-908.
 17. Yun, S., Im, H., Heo, Y., Kim, J. (2011). Crosslinked sulfonated poly(vinyl alcohol)/sulfonated multi-walled carbon nanotubes nanocomposite membranes for direct methanol fuel cells. *Journal of Membrane Science*, 380, 208-215.
 18. Zhang, Y., Yang, Y., Tang, K. (2007). Physicochemical characterization and antioxidant activity of quercetin-loaded chitosan nanoparticles yuying. *Polymers & Polymer Composites*, 21, 449-456.
 19. Mo, S., Peng, L., Yuan, C., Zhao, C., Tang, W. et al. (2015). Enhanced properties of poly(vinyl alcohol) composite films with functionalized graphene. *RSC Advances*, 5, 97738-97745
 20. Rhim, J.W., Park, H. B., Lee, C. S., Jun, J. H., Kim, D. S. et al. (2004). Crosslinked poly(vinyl alcohol) membranes containing sulfonic acid group: proton and methanol transport through membranes. *Journal of Membrane Science*, 238, 143-151.
 21. Yun, S., Im, H., Heo, Y., Kim, J. (2011). Crosslinked sulfonated poly(vinyl alcohol)/sulfonated multi-walled carbon nanotubes nanocomposite membranes for direct methanol fuel cells. *Journal of Membrane Science*, 380, 208-215.
 22. Kraysberg, A., Ein-Eli, Y. (2014). Review of advanced materials for proton exchange membrane fuel cells. *Energy & Fuels*, 28, 7303-7330.
 23. Okada, T., Xie, G., Gorseth, O., Kjelstrup, S., Nakamura, N. et al. (1998). Ion and water transport characteristics of Nafion membranes as electrolytes. *Electrochimica Acta*, 43, 3741-3747.
 24. Witt, M. A., Barra, G. M. O., Bertolino, J. R., Pires, A. T. N. (2010). Crosslinked chitosan/poly (vinyl alcohol) blends with proton conductivity characteristic. *Journal of the Brazilian Chemical Society*, 21, 1692-1698.